Transition Probabilities and Collision Broadening Cross Section of the N_2 Lyman–Birge–Hopfield System*

D. E. SHEMANSKY†
Kitt Peak National Observatory,‡ Tucson, Arizona
(Received 16 June 1969)

Bands of the N_2 Lyman–Birge–Hopfield system ($a\,^1\Pi_g$–$X\,^1\Sigma_g^+$) have been observed in absorption in path lengths ranging from 5.6×10^{-3} to 0.5 m·atm. Comparison of theoretical and measured curves of growth and band profiles have allowed the computation of band transition probabilities, lifetimes of the $a\,^1\Pi_g$ state [$\tau(0)=1.4\times10^{-4}$ sec], relative probabilities of electric quadrupole and magnetic dipole components, and a measure of the collision self-broadening cross section ($\sigma=1.6\times10^{-14}$ cm^2).

I. INTRODUCTION

The N_2 Lyman–Birge–Hopfield (LBH) system is a forbidden transition ($a\,^1\Pi_g$–$X\,^1\Sigma_g^+$) falling in the 1000–1450-Å region of the absorption spectrum. The system is of interest to aeronomy, although its importance may have been exaggerated in the earlier theoretical estimates (Green and Barth,[1] cf. Miller *et al.*[2]).

The transition is not difficult to observe in absorption, and a number of observations have been reported in the literature (see Watanabe[3] and Vanderslice *et al.*[4]). However, quantitative absorption measurements are complicated by the compact structure of the bands. A resolution of the order of 300 000 is required to resolve the rotational structure (Wilkinson[5]). Only one determination of the oscillator strengths has been made from absorption measurements (Ching *et al.*[6]). The requirement of a high resolution was eliminated in this experiment by using the technique of pressure broadening in an He–N_2 mixture. However, the lifetimes of the $a\,^1\Pi_g$ state were rendered uncertain by these measurements, since the values calculated from the oscillator strengths are about a factor of 5 shorter than those determined from the time-of-flight measurements of Lichten[7] (1.7×10^{-4} sec) and Olmstead *et al.*[8] (1.2×10^{-4} sec).

The analysis of recent low-pressure absorption measurements of the LBH system is presented in this article. The spectra, like those of Ref. 6, were too low in resolution to separate the rotational structure. For this reason the observations were limited to the strong regions of the curves of growth. The use of a theoretical model was therefore necessary for the determination of reasonably accurate transition probabilities. The uncertainty in not using this approach would be enhanced in this case because of the mixed nature of the transition; the ($a\,^1\Pi_g$–$X\,^1\Sigma_g^+$) transition is composed of comparable contributions of the magnetic dipole and electric quadrupole moments (Wilkinson and Mulliken[9]). The lifetime of the $a\,^1\Pi_g$ state determined from the measured equivalent widths, in the strong absorption case, depends to a measurable degree on the relative contributions of the two moments. Given the available data, the relative moments could be determined only through the use of a model.

The lifetimes of the levels of the $a\,^1\Pi_g$ state calculated from measurements of the (0, 0) through (6, 0) bands [$\tau(0)=1.4\times10^{-14}$ sec] are in good agreement with the time-of-flight measurements. The source of the discrepancy with the Ching *et al.* measurements is not obvious. A reinterpretation of their experimental results suggests no measureable variation in transition probability over the applied range of total pressures (2500–30 000 torr). If the measurements are valid, the transition probability must then have a peculiar dependence on He pressure that cannot be explained simply in terms of a pressure-induced moment. Both sets of measurements indicate no measurable variation of the electronic transition moment, in agreement with the observations in emission by McEwen.[10]

The measured fraction of the transition probability due to the electric quadrupole moment [0.10 for the (5, 0) band] is in fair agreement with the original rough estimate of Wilkinson and Mulliken,[9] but disagrees by a factor of 2 with the more recent measurements of Vanderslice *et al.*[11] A possible explanation of this discrepancy will be discussed below.

A measure of the collisional self-broadening cross section has been obtained by comparison with a model based on a Voigt line profile. The cross section ($1.6\times$

---

* Contribution No. 483 from the Kitt Peak National Observatory.
† Present address: Dept. of Physics, Univ. of Pittsburgh, Pittsburgh, Pa.
‡ Operated by the Association of Universities for Research in Astronomy, Inc., under contract with the National Science Foundation.

[1] A. E. S. Green and C. A. Barth, J. Geophys. Res. **70**, 1083 (1965).
[2] R. E. Miller, W. G. Fastie, and R. C. Isler, Technical Report No. 13, Johns Hopkins University, Department of Physics, September 1967.
[3] K. Watanabe, Advan. Geophys. **5**, 185 (1958).
[4] J. T. Vanderslice, S. G. Tilford, and P. G. Wilkinson, Astrophys. J. **141**, 395 (1965).
[5] P. G. Wilkinson, Astrophys. J. **126**, 1 (1957).
[6] B. K. Ching, G. R. Cook, and R. A. Becker, J. Quant. Spectry. Radiative Transfer **7**, 323 (1967).
[7] W. Lichten, J. Chem. Phys. **26**, 306 (1956).
[8] J. Olmsted III, A. S. Newton, and K. Street, J. Chem. Phys. **42**, 2321 (1955).
[9] P. G. Wilkinson and R. S. Mulliken, Astrophys. J. **126**, 10 (1957).
[10] D. J. McEwen, Ph.D. thesis, University of Western Ontario, 1965.
[11] J. T. Vanderslice, P. G. Wilkinson, and S. G. Tilford, J. Chem. Phys. **42**, 2681 (1965).

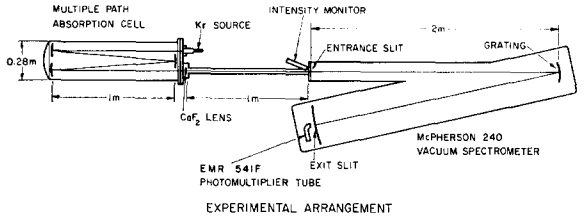

FIG. 1. Experimental arrangement.

10^{-14} cm^2) is 13 times larger than the value determined from kinetic theory.

II. EXPERIMENT

The experimental arrangement is essentially the same as that described by Shemansky.[12] A schematic diagram of the system is shown in Fig. 1. The absorption tube was a modified 1-m Perkin–Elmer multiple path cell. A path length of 4 m was used for all of the measurements presented here. The analyzing instrument was a 2-m McPherson 240 vacuum spectrometer, with a 600-lines/mm grating. The resolution of the instrument was limited to about 15 000, with 10-μ entrance and exit slits. However, most of the observations were made with a 50-μ entrance slit in order to obtain an increased signal. The signal, limited by the transmission of the absorption cell, was impaired by a gradual deposition of photodissociated diffusion pump oil on the reflecting and transmitting surfaces. This difficulty was eliminated for the later measurements of the N_2 Vegard–Kaplan system discussed in Ref. 12. The large dynamic range required for the measurements was obtained through the use of photomultiplier tubes in the pulse counting mode. The continuum source was a krypton-filled tube with a LiF window, excited by a 100-W microwave generator.

The absorption cell was filled with purified Matheson research grade N_2, to pressures varying from 1 to 100 torr, giving path lengths between 5.6×10^{-3} and 0.5 m·atm.

Curves of growth of seven bands, (0, 0) through (6, 0), over the above range of pressures were obtained using reduction procedures similar to those described in detail in Ref. 12. The accuracy of the measured equivalent widths is slightly less than that obtained in the later measurements of Ref. 12, due to the lack of open structure in the observed bands. Measurements on the (0, 0), (1, 0), and (4, 0) bands were complicated by contamination with bands of an unidentified impurity. Figure 2 shows a spectrum $(1-I_\nu/I_0)$ of the (2, 0) band obtained at a pressure of 1.06 torr, in comparison with a synthetic spectrum. The weak feature at $\nu=72\,283$ cm^{-1} is the S branch of the quadrupole component of the transition. The remaining branches are not separable at this resolution (15 000). The remaining bands are similar in shape with moderate differences in the relative intensity of the quadrupole branches. The spectra will be discussed further in Sec. IV.

[12] D. E. Shemansky, J. Chem. Phys. **51**, 689 (1969).

III. THEORY

A. Characteristics of the Transition

The observations presented in this article were made primarily to obtain quantitative measures of the transition probabilities. The determination of these quantities from the absorption measurements requires knowledge of the fine structure of the bands. The following discussion of the band structure will therefore be restricted to this purpose.

The $(a\,^1\Pi_g$–$X\,^1\Sigma_g^+)$ transition has five branches, O, P, Q, R, and S. The P, Q, and R branches arise from the combined magnetic dipole and electric quadrupole moments. The O and S branches are pure quadrupole transitions. The line strength factors have been calculated theoretically by Chiu.[13] These factors are repeated in Table I, since Chiu's notation leads to erroneous branch designations (see Appendix A).

The bands of this system can be characterized by single well-defined transition probabilities $(A_{v'v''})$, since the total rotational transition probabilities $(A_{J'})$ are very nearly independent of the quantum number J' (see the more detailed discussions of Refs. 12 and 14). The quantity $A_{J'}$ is related to the transition probabilities of the rotational lines of a given band by the equation

$$A_{J'}=\sum_{J''}A_{J'J''}. \tag{1}$$

In this case,

$$A_{v'v''}=A_{J'}. \tag{2}$$

The transition probability $A_{J'J''}$ is related to the absorption probability $(B_{J''J'})$ by the equation

$$A_{J'J''}=4\pi hc(\nu_{J'J''})^3(d_{J''}/d_{J'})B_{J''J'}, \tag{3}$$

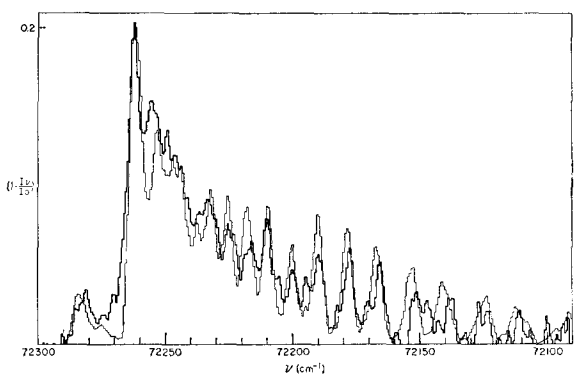

FIG. 2. Comparison of calculated and observed N_2 LBH (2, 0) band, $[1-(I_\nu/I_0)]$ vs ν. $P=1.06$ torr; $T=295.4$°K; $l=403$ cm; $\Delta\nu=3.9$ cm^{-1}. Heavy trace: experimental spectrum: $W_{2,0}=8.6$ cm^{-1}; $[1-(I_\nu/I_0)]_{\text{Peak}}=0.21$. Light trace: synthetic spectrum: $W_{2,0}=8.6$ cm^{-1}; $D_1^2=8.0\times10^{-42}$ erg·cm^3; $Q_1^2/D_1^2=8.5\times10^{-12}$ $[1-(I_\nu/I_0)]_{\text{Peak}}=0.202$.

[13] Y. N. Chiu, J. Chem. Phys. **42**, 2671 (1965).

where $d_{J'}$ and $d_{J''}$ are the rotational degeneracies of the upper and lower states, respectively. The symbol ν refers to wavenumber (cm^{-1}) throughout this article. In contrast to Eq. (4) of Ref. 14, Eq. (3) includes the degeneracy of the upper state due to Λ-type doubling, although the rotational levels of the $a\,{}^1\Pi_g$ state are actually split. This formalism is adopted simply to be consistent with the synthetic spectrum computations, which do not take the splitting into account. Thus the transition probability of a band is determined by summation over all transitions from a given upper-state rotational level:

$$A_{v'v''}={}^4A_{v'v''}+{}^2A_{v'v''}$$
$$=(C4)Q_1^2\sum_{J''}[(\nu_{J'J''})^5({}^4S_J)/2J'+1]$$
$$+(C2)D_1^2\sum_{J''}[(\nu_{J'J''})^3({}^2S_J)/2J'+1], \quad (4)$$

where ${}^4S_J$, ${}^2S_J$ are the line strength factors and Q_1, D_1 are the vibronic matrix elements of the electric quadrupole and magnetic dipole components, respectively; $C4=32\pi^6/5h$ and $C2=64\pi^4/3h$. Equation (4) reduces to

$$A_{v'v''}=\tfrac{4}{3}(C4)(\nu_{v'v''})^5Q_1^2+2(C2)(\nu_{v'v''})^3D_1^2, \quad (5)$$

using the line strength factors in Table I. Similarly,

$$B_{v''v'}=(2\pi hc)^{-1}[(C4)\tfrac{2}{3}(\nu_{v'v''})^2Q_1^2+(C2)D_1^2]. \quad (6)$$

The transition and absorption probabilities of the bands are thus related to the vibronic matrix elements, which in turn determine the transition and absorption probabilities of each rotational transition within the bands.

The transition probabilities of the bands of most electronic transitions can be related by the well-known equation

$$A_{v'v''}=\nu_{v'v''}{}^3R_e^2(\bar{r})q_{v'v''}, \quad (7)$$

where $R_e(\bar{r})$ is the electronic transition moment and $q_{v'v''}$ is the Franck–Condon factor. The vibronic matrix elements are therefore related to $R_e(\bar{r})$ through the Franck–Condon factors

$$R_e^2(\bar{r})=\tfrac{4}{3}(C4)\nu_{v'v''}{}^2Q_1^2/q_{v'v''}+2(C2)D_1^2/q_{v'v''}. \quad (8)$$

TABLE I. Line strength factors of ${}^1\Pi\leftrightarrow{}^1\Sigma$ transitions.[a]

${}^1\Sigma$–${}^1\Pi$	${}^1\pi$–${}^1\Pi$	S_J
		Quadrupole
$S(J)$	$O(J+2)$	$4(J+2)J/3(2J+3)$
$R(J)$	$P(J+1)$	$2(J+2)/3$
$Q(J)$	$Q(J)$	$2(2J+1)/(2J-1)(2J+3)$
$P(J)$	$R(J-1)$	$2(J-1)/3$
$O(J)$	$S(J-2)$	$4(J-1)(J+1)/3(2J-1)$
		Dipole
$R(J)$	$P(J+1)$	J
$Q(J)$	$Q(J)$	$2J+1$
$P(J)$	$R(J-1)$	$J+1$

[a] See Appendix A, Chiu.[13]

[14] D. E. Shemansky and N. P. Carleton, J. Chem. Phys. 51, 682 (1969).

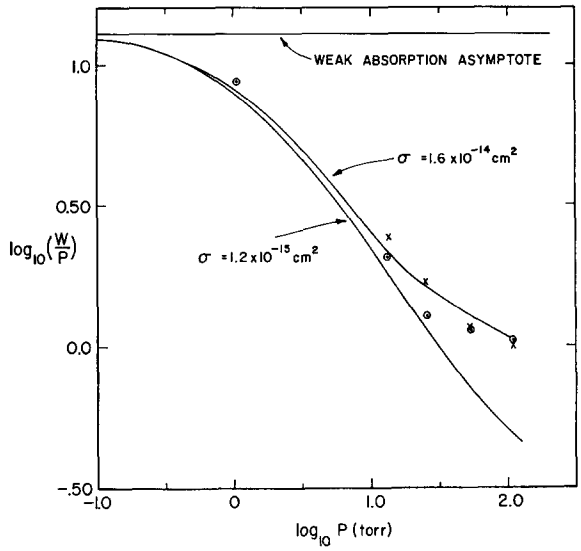

FIG. 3. Log W/P vs log P for the N_2LBH (2, 0) and (3, 0) bands. Experimental: ○, (2, 0) band; ×, (3, 0) band; $l=403$ cm. Theoretical: smooth curves—$D_1^2=7.6\times10^{-42}$ erg cm³, (2, 0) band; $D_1^2=7.3\times10^{-42}$ erg cm³, (3, 0) band; $Q_1^2/D_1^2=8.5\times10^{-12}$; Upper curve—$\sigma=1.6\times10^{-14}$ cm²; Lower curve—$\sigma=1.2\times10^{-15}$ cm².

B. Transition Probabilities from Absorption Spectra

The absorption coefficient (k_ν) is defined by the equation

$$I_\nu=I_0\exp(-k_\nu l), \quad (9)$$

where I_ν is the transmitted intensity, I_0 is the incident intensity, and l is the thickness of the absorbing gas. The absorption probability of a line is related to k_ν through the equation for the integrated band strength (cf. Ref. 12),

$$S_{v''v'}=\sum_{J'}\sum_{J''}S^{J''J'}$$
$$=\sum_{J'}\sum_{J''}\int k_\nu{}^{J''J'}d\nu$$
$$=\sum_{J'}\sum_{J''}h\nu_{J''J'}B_{J''J'}N_{J''}, \quad (10)$$

where $N_{J''}$ is the population of rotational level J''. Equations (9) and (10) can thus be combined to relate the absorption probability to the equivalent width:

$$W_{v'v''}=\sum_{J''}\sum_{J'}\int\left[1-\left(\frac{I_\nu{}^{J''J'}}{I_0}\right)\right]d\nu. \quad (11)$$

The evaluation of Eq. (9) in the strong absorption case requires knowledge of k_ν as a function of ν. At pressures in the 1-torr region the line profiles are well defined by the kinetic motion of the molecules. However, at higher pressures the profiles are modified by collision broadening. This process is not as well understood and requires the introduction of two assumptions. The synthetic spectra computed here were based on an assumed Lorentz collision broadening profile. It

TABLE II. Transition probabilities of the observed $N_2 a\ ^1\Pi_g - X\ ^1\Sigma_g^+$ bands.

Band	ν	$D_1^2 \times 10^{42}$ [a] (erg·cm³)	$^4A_{v'v''}/^2A_{v'v''}$	$A_{v'v''}$ [b] (sec^{-1})	$A_{v'v''}$ [c] (sec^{-1})	Deviation[d]
0, 0	68 965	1.5	0.08	3.3+2	4.0+2	1.2
1, 0	70 612	6.7	0.084	1.60+3	1.16+3	0.73
2, 0	72 250	7.6	0.088	1.96+3	1.85+3	0.94
3, 0	73 861	7.3	0.092	2.02+3	2.13+3	1.06
4, 0	75 444	8.0	0.096	2.36+3	1.99+3	0.84
5, 0	76 995	4.9	0.10	1.54+3	1.61+3	1.04
6, 0	78 527	3.7	0.104	1.24+3	1.17+3	0.94

[a] $Q_1^2/D_1^2 = 8.5 \times 10^{-12}$.
[b] Computed from measured D_1^2.
[c] Proportional to Franck–Condon factors, based on weighted average of Column 5 [W. Benesh, J. T. Vanderslice, S. G. Tilford, and P. G. Wilkinson, Astrophys. J. **143**, 236 (1966).
[d] Column 6/Column 5.

was further assumed that the broadening coefficient was not dependent on the quantum number J. The computational methods of Armstrong[15] were used to determine the convolution of Doppler and Lorentz line shapes (Voigt function).

IV. DISCUSSION

A. Reduction of the Measurements

The equivalent width of a band in strong absorption depends on the relative and absolute transition probabilities, profiles, and effective numbers of the lines that make up the fine structure. There is also a dependence on line spacing, in this case, since the pressure-broadened lines overlap to a considerable degree in the head region at the higher pressures. These factors are combined in the model calculations to produce synthetic comparison spectra.

In order to determine the transition probability of a band from the experimental data, one requires a measure of the integrated band strength ($S_{v''v'}$). This quantity cannot be recovered directly from the observed spectra due to the convolution of I_ν with the very broad instrumental function. The only available data are the equivalent width, which is independent of the instrumental function, and the profile of the convolved spectrum. The analysis of the spectra therefore requires an iterative computation using a model containing a number of parameters.

The first step in the iterative process was to determine the initial values of Q_1^2 and D_1^2, and to fix the ratio Q_1^2/D_1^2. This measurement was made at the lowest pressure in order to approach the Doppler profile as closely as possible, and to obtain a maximum sensitivity of the equivalent widths of the S branch and the remainder of the band to the ratio Q_1^2/D_1^2. Figure 2 shows the final synthetic spectrum of the (2, 0) band calculated for a Doppler line profile and an assumed triangular instrumental function, in comparison with an experimental spectrum obtained at about 1 torr (5.6×10^{-3} m·atm). The values of Q_1^2 and D_1^2 determined from the comparison of synthetic and experimental spectra could not immediately be accepted as valid numbers, since the assumption of a Doppler line profile may not have been a valid one. However, it will be shown that the line profiles at 1 torr are effectively due to the Doppler effect.

For a given path length and pressure, one can obtain the same equivalent width for a range of combinations of the parameters Q_1^2 and D_1^2 and the Lorentz broadening coefficient (α_L). In general, these quantities would not be easily separated, without a direct measurement of α_L, even with measurements over a range of pressures. The profile of the band limits the uncertainty to some degree, but the relative intensities of the features in a band in strong absorption are also a function of all three parameters. Thus the estimated ratio (Q_1^2/D_1^2) in the low-pressure case shown in Fig. 2 is an upper limit of the real value since the minimum possible linewidth was used in the computation. In this particular case the analysis is simplified considerably by the low magnitude of the measured upper limit ($Q_1^2/D_1^2 = 8.5 \times 10^{-12}$). The small contribution from the quadrupole transition that this represents makes the calculated equivalent width quite insensitive to a possible large error in the estimated value of the ratio. The transition probability of a band could then be separated from the broadening coefficient in the usual manner by comparing calculated and measured curves of growth.

Figure 3 shows the nearly identical plots of $\log W/P$ vs $\log P$, where P is pressure, of the (2, 0) and (3, 0) bands. A measure of the error in the measured equivalent widths can be obtained from the scatter between the two sets of values. This is due mostly to errors in the estimation of I_0, which could be partly systematic. The figure shows two calculated curves of growth having the same values of Q_1^2 and D_1^2, but differing in the value of the pressure broadening coefficient. The lower curve corresponds to a broadening cross section (σ) equal to the gas-kinetic value and the upper curve is the estimated best fit to the measured equivalent widths. The estimated broadening cross section ($\sigma = 1.6 \times 10^{-14}$ cm²) is 13 times larger than the gas-kinetic value. As one might infer from the convergence of the

[15] B. H. Armstrong, J. Quant. Spectry. Radiative Transfer **7**, 61 (1967).

TABLE III. N_2 Lyman–Birge–Hopfield absolute transition probabilities.[a]

v' \ v''	0	1	2	3	4	5	6	7	8	9	10	11	12	13	14	15	16	17	18	19	20	$A_{v'}$	τ
0	1450 403	1501 1280	1555 1873	1612 1678	1672 1034	1736 462	1805 156	1878 49	1956 9	2041 1	2130 —											6936	1.44 − 4
1	1416 1164	1464 1751	1515 650	1570 4	1627 550	1688 [illegible]	1752 [illegible]	1821 [illegible]	1895 267	1973 43	2057 9	2147 1										6846	1.46 − 4
2	1384 1848	1430 346	1479 30	1530 856	1581 [illegible]	1642 3	1703 [illegible]	1768 [illegible]	[illegible]	[illegible]	[illegible]	[illegible]	[illegible]	[illegible] 1								[illegible]	1.48 − 4
3	1354 2126	1398 129	1444 718	1493 585	1545 32	[illegible] 665	[illegible] 390	1715 3	[illegible] 417	1854 724	[illegible] 541	2007 242	[illegible] 73	[illegible] 16	[illegible] 2	[illegible] —						[illegible]	1.50 − 4
4	1325 1989	1368 70	1412 980	1459 4	1508 647	1560 264	1616 127	1674 583	1736 175	1801 59	1871 490	1945 616	2025 376	2109 143	2200 37	2297 7	2402 1					6567	1.52 − 4
5	1299 1611	1339 560	1382 507	1427 339	1474 496	1523 75	1576 569	1631 41	1690 297	1752 432	1818 24	1888 192	1953 536	2042 477	2127 231	2218 72	2315 16	2420 2	2532 —			6478	1.54 − 4
6	1273 1171	1312 1085	1353 53	1396 766	1441 24	1489 550	1539 103	1592 301	1648 330	1707 20	1769 413	1835 208	1906 16	1981 349	2060 503	2145 323	2236 124	2333 31	2438 5	2550 1		6375	1.57 − 4
7	1249 790	1287 1353	1326 71	1367 632	1411 182	1456 423	1504 118	1555 427	1608 13	1664 418	1723 65	1786 185	1853 356	1923 29	1998 144	2078 437	2164 342	2255 186	2352 55	2456 11	2568 2	6282	1.59 − 4
8	1227 501	1263 1337	1301 444	1340 217	1382 587	1426 36	1472 495	1520 30	1571 382	1624 97	1681 210	1740 265	1804 14	1870 332	1941 159	2017 19	2097 305	2182 414	2273 250	2370 90	2474 71	6203	1.61 − 4
9	1206 299	1240 1126	1277 850	1315 1	1355 630	1397 105	1441 366	1497 152	1536 285	1587 101	1641 307	1698 16	1759 330	1821 38	1886 174	1960 274	2035 11	2115 157	2201 383	2292 308	2389 132		
10	1185 174	1219 859	1254 1091	1291 134	1329 337	1370 447	1412 44	1456 445	1503 4	1552 378	1603 6	1658 316	1715 44	1775 206	1839 175	1906 32	1978 286	2054 90	2134 43	2220 303	2311 340		
11	1165 97	1199 600	1233 1108	1268 457	1305 55	1344 578	1385 61	1427 323	1472 171	1519 181	1568 187	1620 153	1675 135	1732 197	1795 45	1857 261	1925 6	1997 196	2073 188	2153 —	2239 197		
12	1148 54	1179 404	1212 997	1247 772	1282 18	1320 406	1359 341	1400 50	1443 402	1488 —	1536 334	1585 11	1638 285	1692 5	1750 266	1811 4	1876 219	1944 84	2016 75	2092 238	2172 28		
13	1130 29	1161 258	1193 905	1226 952	1261 211	1297 137	1335 519	1374 34	1416 294	1459 163	1505 116	1552 239	1602 53	1655 227	1710 49	1768 192	1839 31	1904 98	1963 178	2035 5	2111 213		
14	1114 15	1144 157	1174 598	1207 963	1240 487	1275 2	1312 433	1350 254	1390 57	1432 363	1476 5	1521 278	1569 50	1620 200	1673 70	1728 172	1787 50	1848 189	1913 10	1982 209	2054 17		
15	1098 8	1127 95.0	1157 426	1188 881	1221 724	1255 70	1290 214	1327 448	1366 15	1406 272	1448 160	1492 74	1538 255	1587 9	1639 244	1691 —	1747 220	1806 1	1867 197	1933 15	2001 153		

Key: v'' across, v' down; each cell: λ / $A_{v'v''}$ (sec^{-1})

[a] Franck–Condon factors from Benesch *et al.*[17]

two curves of Fig. 3 in the 1-torr region, there is very little difference between a line broadened only by the Doppler effect and the Voigt profile in 5.6×10^{-3} m·atm of gas. The upper limit estimate of Q_1^2/D_1^2 discussed above is therefore equal to the actual value of the ratio.

The values of D_1^2 and $A_{v'v''}$ calculated from the observed curves of growth for the (0, 0) through (6, 0) bands are given in Table II. There was no measurable variation of either the collision broadening coefficient or the Q_1^2/D_1^2 ratio as a function of vibrational quantum number (v'). The variation in the ratio ${}^4A_{v'v''}/{}^2A_{v'v''}$ given in the table is thus entirely due to the energy differences of the transitions. The sixth column in the table is an improved set of $A_{v'v''}$ values based on the Franck–Condon factors for the transitions. The electronic transition moment was assumed to be virtually a constant, with a small dependence on the energy of the transition, stemming from the energy-dependent contribution of the quadrupole moment; it was assumed that the ratios $Q_1^2/q_{v'v''}$ and $D_1^2/q_{v'v''}$ did not vary from band to band [Eq. (8)]. The deviations of the experimental values from the improved set clearly suggest this is the case, in agreement with the absorption measurements of Ref. 6 and the emission measurements of McEwen.[10] The magnitudes of the deviations are of the order of 10% with the exception of the bands blended with impurity features. Having thus obtained a measure of the electronic transition moment, one can compute a complete table of absolute $A_{v'v''}$ values and hence determine the lifetimes of the system. These quantities are given in Table III. The calculated lifetimes increase slowly from $\tau(0)=1.4\times10^{-4}$ sec for the $v'=0$ level to $\tau(8)=1.6\times10^{-4}$ sec for the $v'=8$ level.

The accuracy of the measured equivalent widths is estimated to be roughly 10%. This corresponds to probable errors of about 30% for the calculated transition probability and 30% for the collision broadening coefficient at the highest pressure, for a single equivalent width measurement. The accuracy of the transition probabilities are somewhat improved by the use of curves of growth, since one is, in effect, averaging a number of measurements. The probable error of the calculated lifetimes is thus estimated to be about 20%. The use of the curves of growth does not measurably improve the accuracy of the collision broadening coefficient since the probable error goes up with decreasing pressure. The band profiles do not provide an improved measure of α_L in this case due to the low resolution of the high-pressure spectra.

B. Comparison with Other Measurements

The lifetimes given in Table III are in good agreement with the time-of-flight measurements of Lichten[7] ($\tau=1.7\times10^{-4}$ sec) and Olmsted *et al.*[8] ($\tau=1.2\times10^{-4}$ sec). There is some uncertainty in the Lichten estimate in that the metastable species in his experiment were not directly identified as molecules in the $a\ {}^1\Pi_g$ state. The absorption measurements of Ching *et al.*[6] yield about the same relative transition probabilities as the present measurements, but the lifetimes calculated from their oscillator strengths are a factor of 5 shorter than the values in Table III. The experimental method of Ref. 6 was to pressure broaden the lines with a high-pressure He–N_2 mixture in order to obtain a measure of the integrated band strength [Eq. (10)] directly from the observed profile of the band. The measurements were made with total pressures up to 700 psi (36 000 torr). The measurements were characterized by a rapid rise in the apparent absorption probability as a function of total pressure up to a pressure of about 200 psi, where the curves leveled off to form a slightly rising plateau. The oscillator strengths were estimated by extrapolating the plateau regions of the curves to

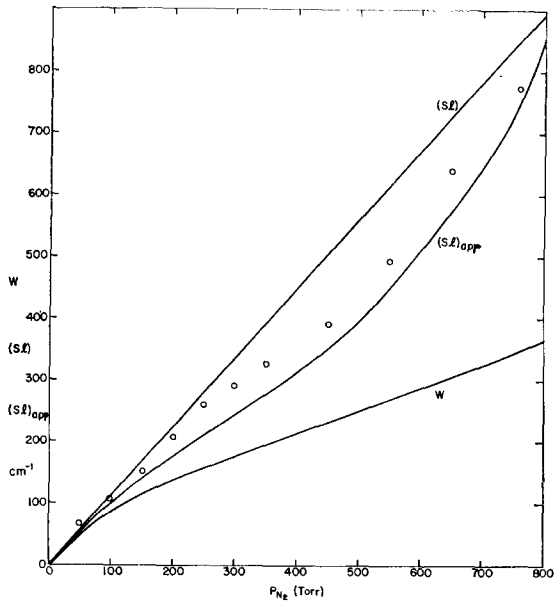

FIG. 4. W, (Sl), $(Sl)_{app}$ vs P_{N_2} calculated from the Ching *et al.*[6] measurements. O, Experimental measurements, $(Sl)_{app}$ of Ref. 6.

zero pressure. Ching *et al.* apparently assumed that the slowly rising portion of the curve represented pressure dependence of the transition probability. However, it can be shown that they very likely misinterpreted the experimental measurements through the assumption that the widths of the line profiles were similar in width to the instrumental function. One can place an upper limit on the linewidths in the observed bands by estimating the degree of saturation in the absorption. The results presented by Ching *et al.* suggest values an order of magnitude smaller than the instrumental width. The integrated band strengths calculated from the band profiles would then be only apparent values, somewhere between the equivalent width and the real integrated band strength. The experimental results can in fact be reproduced by assuming a constant transition probability over the entire range of total pressures (2500–30 000 torr). Details of the calculation are given in Appendix B. The plateau region of the apparent absorption probability curve, which Ching *et al.* interprets as a variation in transition probability, must actually be the curve of desaturation of the bands according to the present interpretation. The sharply rising portion of the curve is due to the dependence of the apparent integrated band strength on the equivalent width, caused by the smearing of the spectrum by the broad instrumental profile. The effect of the reinterpretation of the Ching *et al.* experiment is to raise the estimated transition probability (~10% for the 3, 0 band) and thus increase the divergence with the present work.

If one accepts both sets of measurements, this suggests a peculiar dependence on He pressure that cannot be explained simply in terms of a pressure-induced dipole or quadrupole moment. Further discussion should clearly await additional measurements at lower pressures in He–N_2 mixtures.

Two earlier estimates of the relative electric quadrupole and magnetic dipole transition probabilities have been published (Wilkinson and Mulliken[9] and Vanderslice *et al.*[11]). The ratio ${}^4A_{5,0}/{}^2A_{5,0}=0.15$ obtained by Ref. 9 is in fair agreement with the value (0.10) obtained here. However, little weight should be placed on the comparison because of the very crude nature of the former estimate. The measurements of Ref. 11 represent an attempt to obtain an improved value over that of Ref. 9. These measurements were made by comparing equivalent widths of lines, using photographic spectra. The accuracy was limited in this case, not only by the dynamic range of the photographic film, but also by the long path length of the observation (~0.4 m·atm, 15 torr, Tilford[16]). This placed the spectra far into the region of strong absorption. The comparisons of the strong mixed transition lines with the weaker quadrupole lines were therefore subject to a severe limitation in accuracy. The ratio (0.33) given by Ref. 11 is not actually a measure of the relative transition probabilities, since the line strength factors alone were used in the computation rather than the line absorption probabilities (Tilford[16]). However, the ratio Q_1^2/D_1^2 as defined here can be derived from this quantity. This value ($Q_1^2/D_1^2=1.9\times10^{-11}$) is about a factor of 2 greater than the number given in Table II. An error this large in the measurement of Ref. 11 would not be unexpected (Tilford[16]).

The author is not aware of previous measurements of the collision broadening cross section.

V. CONCLUSIONS

Measurements of the absorption spectrum of the N_2 LBH system have allowed the computation of transition probabilities of the bands and lifetimes of the $a\,{}^1\Pi_g$ state [$\tau(0)=1.4\times10^{-6}$ sec]. The use of synthetic comparison spectra has in addition allowed measurements of the relative contributions of the electric quadrupole and magnetic dipole moments ($Q_1^2/D_1^2=8.5\times10^{-12}$), and the collision broadening cross section. The ratio Q_1^2/D_1^2 appears to be constant from band to band, within the accuracy of measurement (~20%). Furthermore, the electronic transition moment [$R_e(\bar{r})$], which is proportional to the ratios $(Q_1^2/q_{v'v''})^{1/2}$ and $(D_1^2/q_{v'v''})^{1/2}$, does not vary measurably from band to band. This is in agreement with earlier measurements (Refs. 6 and 10). The collision broadening cross section ($\sigma=1.6\times10^{-14}$ cm^2), which is based on an assumed Lorentz broadening profile, is a factor of 13 larger than the kinetic collision cross section. The cross section appears to be constant from band to band within the measurement accuracy (~30%).

[16] S. G. Tilford (private communication).

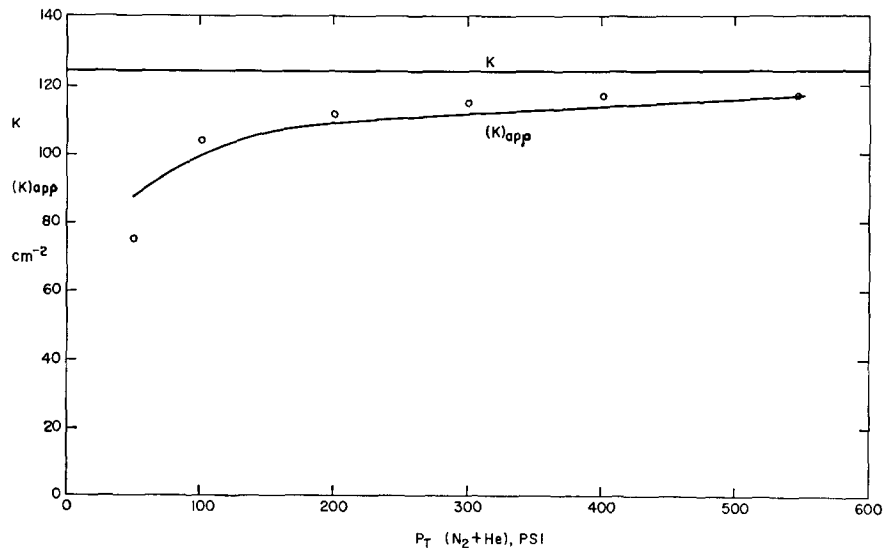

FIG. 5. K, $(K)_{app}=(S)_{app}N_0/N$ vs P_T calculated from the Ching *et al.* measurements. O, Experimental measurements, $(K)_{app}$, of Ref. 6.

The present estimate of the lifetimes of the $a\,^1\Pi_g$ state is in good agreement with the time-of-flight measurements of Refs. 7 and 8. However, the high-pressure absorption measurements of Ching *et al.*[6] in He–N_2 mixtures indicate a lifetime shorter by a factor of 5. The source of this discrepancy is far from obvious, since the present reinterpretation of the Ching *et al.* measurements suggests no variation in transition probability over the 2500–30 000-torr pressure range. The relative transition probabilities due to the electric-quadrupole and magnetic dipole moments ($^4A_{5,0}/^2A_{5,0}=0.10$) is only in rough agreement with the earlier measurements (Refs. 9 and 11). However, a high degree of accuracy was not expected to obtain from the latter due to the use of photographic film, and the high degree of saturation of the observed bands.

Further observations of the ($a\,^1\Pi_g$–$X\,^1\Sigma_g^+$) system in absorption to examine the pressure dependence of the transition probability would be of interest, especially in view of the discrepancy between Ching *et al.* and the present measurements.

APPENDIX A: DESIGNATION OF LINE STRENGTH FACTORS

Chiu[13] does not designate his theoretical line strength factors in the conventional manner. The branch designations are given in terms of initial and final states of the transition, rather than in relation to the relative energies of the states (i.e., upper and lower states). The branch designations should in fact be independent of the initial and final states of the transition. Consequently, the branch designations in the second columns of Chiu's line strength factor tables are erroneous in respect to conventional notation. The following table illustrates the differences in notation for one of the line strength factors by a comparison of the notation of Chiu with the conventional notation [see also by Y.-N. Chiu, J. Chem. Phys. (to be published)]:

Notation	Branch designation for a given line strength factor			
	$^1\Pi_f\leftarrow{}^1\Sigma_i(J)$	$^1\Pi_i\rightarrow{}^1\Sigma_f(J)$	$^1\Sigma_f(J)\leftarrow{}^1\Pi_i$	$^1\Sigma_i(J)\rightarrow{}^1\Pi_f$
Chiu	$O(J)$	$S(J-2)$	$S(J-2)$	$O(J)$
Conventional	$O(J)$	$O(J)$	$S(J-2)$	$S(J-2)$

where $S_J=[4J(J-2)/3(2J-1)]$, Table I of aforementioned article.

APPENDIX B: REINTERPRETATION OF THE CHING *ET AL.* EXPERIMENT

Ching *et al.*[6] based the analysis of their experimental measurements on the assumption that the instrumental width (0.2 Å) was comparable to the width of the spectral lines. The results indicated a pressure-dependent transition probability. It can be shown that the linewidths are in fact an order of magnitude less than the instrumental width. Consequently, the integrated band strengths calculated directly from the observed spectra would differ from the real integrated band strengths by factors varying with the amount of saturation in the absorption. The experimental results are reproduced in the following analysis by assuming a transition probability independent of pressure; the apparent pressure dependence resulting from the original analysis is due to the dependence of the apparent integrated band strength on the amount of saturation in the absorption.

One can estimate the collision broadening coefficient from the ratio W/Sl, by assuming a Lorentz line shape. Equivalent widths are not given directly by Ref. 6, but Fig. 2(a) of the article shows a spectrum of the (3, 0) band obtained at $P_{N_2}=100$ torr and $P_{(N_2+He)}=100$ psi ($l=6.8$ cm). The scale of the absorption in the spectrum clearly suggests a fair degree of saturation since $(1-I_\nu/I_0)_{Peak}\approx 0.66$. A rough upper limit estimate of W/Sl can be made by approximating the shape of the band with an effective absorption coefficient. A triangular shaped absorption coefficient appears to be a reasonably good approximation, and the calculated ratio [for $(1-I_\nu/I_0)_{Peak}=0.66$] $W/(Sl)_{app}=0.75$, where $(Sl)_{app}$ is the apparent total strength of the band. $(Sl)_{app}$ may deviate from the real quantity (Sl) due to smearing by the instrumental function. In general $W<(Sl)_{app}<Sl$, and therefore $W/(Sl)_{app}$ represents an upper limit of the ratio W/Sl. The ratio $W/Sl=0.75$ corresponds to $1/X=2\pi\alpha_L/(Sl)_{line}=1.45$, where $(Sl)_{line}$ is the average total strength of the lines in the band. The effective number of lines in a band can be calculated from the theoretical model, and is determined to be 43. Thus $(Sl)_{line}=Sl/43$. If we calculate the apparent value of (Sl) from the value of $K=SN_0/N$ given by Ref. 6, $(Sl)_{line}=2.4$ cm^{-1}, and $\alpha_L=0.54$ cm^{-1}. This value of α_L is also an upper-limit estimate because of the functional relationship of W/Sl and X. The instrumental width is 11 cm^{-1} at the wavelength of the (3, 0) band. The values of $(Sl)_{app}$ given in Ref. 6 are therefore not necessarily good approximations to Sl, and could not be independent of the amount of saturation. Since α_L must be at least a factor of 20 less than the instrumental width for $P_T=100$ psi, one can surmise that the shape of the curve of K vs P_T given in Fig. 4 of Ref. 6 must be at least partly due to the desaturation of the band. To avoid an iterative computation we anticipate the real value of K as 5% greater than the largest value given in Fig. 4 (Ref. 6), in order to make an improved estimate of W/Sl. This gives $Sl=110$ cm^{-1} for $P_{N_2}=100$ torr. The estimated value of W from Fig. 2(a) (Ref. 6) results in a ratio $W/Sl=0.57$. Another estimate of W/Sl can be obtained by determining the ratio $(Sl)_{app}/Sl$ from Fig. 4 (Ref. 6), assuming the broadening coefficient to be dominated by the He pressure. For $P_T=100$ psi, $(Sl)_{app}/Sl=0.84$, and $W/Sl=(0.75)(0.84)=0.63$. Using the latter value as the best estimate, we obtain $\alpha_L=0.32$ cm^{-1} ($P_{N_2}=100$ torr, $P_T=100$ psi); the equation for the broadening coefficient can be determined from this value of α_L by applying the cross section for self-broadening given in the present work:

$$\alpha_L=(5.7)(10^{-4})P_{N_2}+5.0\times 10^{-5}P_{He}. \qquad \text{(B1)}$$

The broadening cross section for He represented by Eq. (B1) is about 50% less than the kinetic collision cross section.

Equation (B1) can now be used to predict the experimental results of Figs. 3 and 4 of Ref. 6, assuming a constant transition probability.

Figure 4 shows the Ching *et al.* experimental points, $(Sl)_{app}$ vs P_{N_2}, for $P_T=200$ psi (Fig. 3, Ref. 6). The smooth curves represent the calculated variations of Sl, $(Sl)_{app}$, and W as functions of P_{N_2}. The triangular-shaped absorption coefficient mentioned earlier was used to obtain $(Sl)_{app}$:

$$W/(Sl)_{app}=2\,\frac{[(\ln I_0/I_{\nu_1})-(1-I_{\nu_1}/I_0)]}{[\ln I_0/I_{\nu_1}]^2}, \qquad \text{(B2)}$$

where I_{ν_1} is the peak value of the absorption. The straight line drawn through the experimental points by Ching *et al.* crosses above the origin (not shown in Fig. 4). The $(Sl)_{app}$ curve follows the shape indicated by the experimental points remarkably well. Thus the off-set of the Ching *et al.* line appears to be due to smearing by the instrumental function, rather than systematic experimental error, or variation in transition probability.

The slope of the curve in Fig. 4 (Ref. 6) ($K=SN_0/N$ vs P_{He}) can also be reproduced with a fair degree of accuracy. If we assume $P_{N_2}=100$ torr, then $\alpha_L=0.057+5.0\times 10^{-5}P_{He}$, and $K=7.6S$. If there were no variation in transition probability, K would be independent of P_{He}. However, $(K)_{app}$ and $(S)_{app}$ are obtained rather than K and S, due to smearing by the instrumental function. Figure 5 shows the calculated curve compared to the experimental points. The curve in the plateau region agrees very well with the experimental measurements. There is some deviation at the lower pressure ($\sim$15%), but this could easily be due to the rough approximation of the ratio $W/(Sl)_{app}$. The experimental measurements can thus be explained in terms of desaturation of the absorption, rather than a variation in transition probability.